THE JOURNAL OF BIOLOGICAL CHEMISTRY VOL. 286, NO. 16, pp. 14410–14418, April 22, 2011

Double Anti-angiogenic and Anti-inflammatory Protein Valpha Targeting VEGF-A and TNF-α in Retinopathy and Psoriasis*[S]

Received for publication, February 4, 2011 Published, JBC Papers in Press, February 23, 2011, DOI 10.1074/jbc.M111.228130

Keehoon Jung[‡§1], Donghun Lee[¶1], Hye Song Lim[‖], Sang-Il Lee[‖], Yeon Jung Kim[**], Gyun Min Lee[**], Sun Chang Kim[**], and Gou Young Koh[‡§‡‡2]

From the [‡]National Research Laboratory for Vascular Biology and Stem Cells, [§]Graduate School of Biomedical Science and Engineering, [**]Department of Biological Sciences, and [‡‡]Graduate School of Nanoscience and Technology, Korea Advanced Institute of Science and Technology (KAIST), Daejeon 305-701, Korea, the [¶]Department of Dermatology, Seoul National University College of Medicine, Seoul 110-744, Korea, and the [‖]Department of Internal Medicine and Institute of Health Science, Gyeongsang National University School of Medicine, Jinju 660-702, Korea

Pathological angiogenesis usually involves disrupted vascular integrity, vascular leakage, and infiltration of inflammatory cells, which are governed mainly by VEGF-A and TNF-α. Although many inhibitors targeting either VEGF-A or TNF-α have been developed, there is no single inhibitor molecule that simultaneously targets both molecules. Here, we designed and generated a novel chimeric decoy receptor (Valpha) that can simultaneously bind to VEGF-A and TNF-α and block their actions. In this experimental design, we have shown that Valpha, which is an effective synchronous blocker of VEGF-A and TNF-α, can drastically increase treatment effectiveness through its dual-blocking characteristics. Valpha contains the VEGF-A-binding domain of VEGFR1, the TNF-α-binding domain of TNFR2, and the Fc domain of IgG1. Valpha exhibited strong binding characteristics for its original counterparts, VEGF-A and TNF-α, but not for the extracellular matrix, resulting in a highly favorable pharmacokinetic profile *in vivo*. Compared with VEGF-Trap or Enbrel, both of which block either VEGF-A or TNF-α, singularly, Valpha is a highly effective molecule for reducing abnormal vascular tufts and the number of F4/80$^+$ macrophages in a retinopathy model. In addition, Valpha showed superior relief effects in a psoriasis model with regard to epidermal thickness and the area of blood and lymphatic vessels. Thus, the simultaneous blocking of VEGF-A and TNF-α using Valpha is an effective therapeutic strategy and cost-efficient for treatment of retinopathy and psoriasis.

VEGF-A plays a key role in growth, migration, and survival of blood endothelial cells, which are essential processes for angiogenesis, specifically through the activation of VEGFR2 rather than VEGFR1 (1–5). VEGF-A is the prime molecule responsible for tumor and inflammatory angiogenesis, where it promotes abnormal vessel formation and vascular leakage (1, 2, 4–7). Based on this information, many attempts were carried out to block VEGF-A action, including blocking antibody, decoy receptor, aptamer, and siRNA against VEGF-A (8–11). For instance, VEGF-Trap (developed by Regeneron Pharmaceuticals, Inc.) effectively inhibits tumor and ocular angiogenesis and also reduces vascular leakage (9, 12–14). However, VEGF-Trap targets only VEGF-A-related diseases. TNF-α mediates the immune response by recruiting leukocytes to the site of inflammation (15). TNF-α is an important molecule in the initiation of inflammatory responses through activation of NF-κB in the inflammatory cells, including macrophages, endothelial cells, and dendritic cells (16, 17). Several approaches have been developed to block TNF-α action. For instance, Amgen Inc. developed a TNF-α decoy receptor, Enbrel, which is currently being used to treat many inflammatory diseases related to TNF-α (18, 19).

Human VEGFR1 is separated by three major regions: an extracellular domain consisting of seven Ig-like domains, a transmembrane domain, and an intracellular tyrosine kinase domain (20, 21). Ig-like domain 2 (among seven Ig-like domains) of VEGFR1 is essential for VEGF-A binding (20, 21). However, Ig-like domain 2 of VEGFR1 contains many basic amino acids, and its theoretical pI is 9.19 (9, 20). In general, positively charged, high pI proteins bind nonspecifically to the extracellular matrix, which is negatively charged (22). Therefore, Ig-like domain 2 of VEGFR1 *per se* might not be used as a therapeutic protein due to its poor pharmacokinetic properties (9). Human TNFR2 is separated by three major regions: an extracellular domain consisting of four cysteine-rich domains, a transmembrane domain, and an intracellular domain (23, 24). The four cysteine-rich domains of the extracellular domain of TNFR2 are essential for TNF binding (23, 25). Although this subdomain contains many basic amino acids, the theoretical pI of this subdomain is 6.5 because it possesses high amounts of cysteine and other acidic amino acids.

The underlying causes of vision loss in blinding retinal diseases, such as proliferative diabetic retinopathy and age-related macular degeneration, are abnormal and excessive neovascularization and increased vascular permeability (7, 26, 27). However, early vessel loss initiates retinopathy because of an inadequate blood supply resulting from vaso-obliteration, resulting

* This work was supported by National Research Foundation Grant R2009-0079390 (to G. Y. K.), World Class University (WCU) Grant R31-2009-000-10071-0 (to G. Y. K.), and a Korea Advanced Institute of Science and Technology (KAIST) institute grant (2009) funded by the Ministry of Education, Science and Technology, Korea.

[S] The on-line version of this article (available at http://www.jbc.org) contains supplemental "Methods" and Figs. S1–S3.

[1] Both authors contributed equally to this work.

[2] To whom correspondence should be addressed: Graduate School of Biomedical Science and Engineering, KAIST, 373-1 Guseong-dong, Daejeon 305-701, Korea. Tel.: 82-42-350-2638; Fax: 82-42-350-2610; E-mail: gykoh@kaist.ac.kr.

in tissue hypoxia, which determines the severity of subsequent pathological vessel growth (28, 29). Pathological angiogenesis in the retina produces chaotically oriented growth of dysfunctional vessels that grow into the vitreous as vascular tufts and is accompanied by infiltration of various inflammatory cells, including macrophages, leaky vessels, and edema in the retina (26, 29). These pathological features are common in the pediatric retinopathy of prematurity condition and in the diabetic retinopathy of the adult (29). In fact, VEGF-A and TNF-α are simultaneously up-regulated in these pathological retinopathies (1, 26).

Psoriasis is a chronic inflammatory skin disease characterized by marked thickening of the epidermis, tortuous and dilated dermal blood vessels, and characteristic inflammatory cell infiltrates (30, 31). Although the pathogenesis of psoriasis has not been fully elucidated, TNF-α and VEGF-A are overexpressed in psoriasis and are believed to have central roles in the processes (30, 32). In particular, biological agents targeting TNF-α are highly effective in treatment of patients with psoriasis, and VEGF-A blockade has been known to also be effective in mouse models of psoriasis (30–32). To investigate the efficacies of synchronous blockade of VEGF-A and TNF-α, we generated a 12-*O*-tetradecanoylphorbol-13-acetate (TPA)[3]-induced psoriasis model using keratin 14-VEGF-A transgenic mice (33, 34). A mouse psoriasis model using keratin 14-VEGF-A transgenic mice has been validated in several studies and shown to recapitulate many pathological and molecular hallmarks of human psoriasis (31, 33, 34).

Rheumatoid arthritis is a disabling disease that can cause bone destruction and permanent deformity (6, 35). The hallmark of rheumatoid arthritis is synovial cell proliferation in response to inflammatory stimuli, leading to formation of the rheumatoid pannus (6, 35). One of the earliest events observed in synovitis is the development of new vessels in the synovium, and VEGF-A is strongly expressed by subsynovial macrophages, fibroblasts surrounding vessels, vascular smooth muscle cells, and synovial lining cells (6, 36, 37). In human rheumatoid arthritis, VEGF-A is detected in both synovial fluid and serum (35, 37). The VEGF-A expression level in synovial fluid and tissues correlates with the clinical severity of human rheumatoid arthritis and with the degree of joint destruction (35, 36). Among other antirheumatic drugs, TNF-α inhibitors are widely used, and VEGF-A inhibitors have therapeutic potential as well (6, 35, 37).

We hypothesized that double blockade of VEGF-A and TNF-α could be more effective than single inhibition of either VEGF-A or TNF-α in treatment of diseases related to inflammatory angiogenesis. To address our hypothesis, we designed and generated a novel chimeric decoy receptor (Valpha) that can simultaneously bind to VEGF-A and TNF-α and block their actions. Valpha is an effective therapeutic agent for treatment of retinopathy and psoriasis.

[3] The abbreviations used are: TPA, 12-*O*-tetradecanoylphorbol-13-acetate; LEC, lymphatic microvascular endothelial cell; ECM, extracellular matrix; OIR, oxygen-induced retinopathy.

EXPERIMENTAL PROCEDURES

Generation of Recombinant Proteins—Gene constructs encoding human TNFR2 (amino acid residues 23–257), human VEGFR1 (amino acid residues 132–225), and the Fc domain of human IgG (referred to as Fc) were cloned into the pCMV-*dhfr* vector. Recombinant CHO cells expressing Valpha was established following a previously described method (22, 38). Briefly, the cells were established by transfection of a vector containing the *dhfr* (dihydrofolate reductase) and Valpha genes into *dhfr*-deficient CHO cells (CRL-9096, American Type Culture Collection). This was followed by *dhfr*/methotrexate-mediated gene amplification. The stable recombinant CHO cell line secreting the highest amount of Valpha was selected with serially increasing concentrations of methotrexate (0.001–0.32 μM; Sigma). The cells were then grown and maintained in HyQ SFM4CHO (HyClone) supplemented with 1% dialyzed fetal bovine serum (Invitrogen) and 0.32 μM methotrexate. For recombinant Valpha protein production, the cells were inoculated at 2×10^5 cells/ml in 250-ml Erlenmeyer flasks containing 100 ml of medium on an orbital shaker (Vision) at 110 rpm in a humidified 5% CO_2 incubator at 37 °C. After 4 days, the culture media containing recombinant proteins were harvested, and the recombinant Valpha proteins were purified by using protein A-Sepharose affinity chromatography with subsequent acid elution and neutralization. After purification, protein was quantitated using the Bradford assay and confirmed by Coomassie Blue staining of an SDS-polyacrylamide gel.

In Vitro Assays for TNF-α and VEGF-A—To examine the inhibitory activity of Valpha on TNF-α, NF-κB activity was assessed by immunolocalization of p65 in the nuclei of primary cultured lymphatic endothelial cells as described previously (22). Briefly, primary lymphatic microvascular endothelial cells (LECs) derived from adult human dermis were purchased from Cambrex Corp. and maintained in endothelial cell basal medium-2 with growth supplements (EBM-2 MV, Lonza). Passage 4–6 LECs were incubated in EBM-2 MV containing 1% FBS for 8 h and then with 10 μg/ml Fc, VEGF-Trap, Enbrel, or Valpha for 15 min, and the LECs were treated with TNF-α (10 ng/ml) for 30 min. For the immunofluorescence staining of p65, the cells were fixed with 4% paraformaldehyde for 30 min at 4 °C, washed with PBS, permeabilized with PBS containing 0.05% Triton X-100 at 4 °C for 30 min, and then washed with PBS. For blocking, 200 μl of 5% donkey serum was added to each well for 1 h at room temperature. Rabbit anti-human p65 antibody (1:100 dilution; Santa Cruz Biotechnology) was incubated overnight with the cells at room temperature. After incubation of the primary antibody, the cells were washed with PBS and then incubated with donkey anti-rabbit FITC antibody (1:200 dilution; Jackson ImmunoResearch Laboratories) for 2 h at room temperature. For nuclear staining, the cells were incubated with DAPI (1:1000 dilution; Invitrogen) for 10 min. For immunoblotting of p65 nuclear translocalization, the treated LECs were lysed, and their nuclear fractions were collected as follows. The cells were lysed with 10 mM HEPES, 1.5 mM $MgCl_2$, 50 mM KCl, 0.1 mM DTT, and 0.05% Nonidet P-40, and their supernatants were kept as cytosolic fractions. Their pellets were lysed with 5 mM HEPES, 1.5 mM $MgCl_2$, 0.2 mM EDTA, 4.6 M NaCl, 0.5 mM

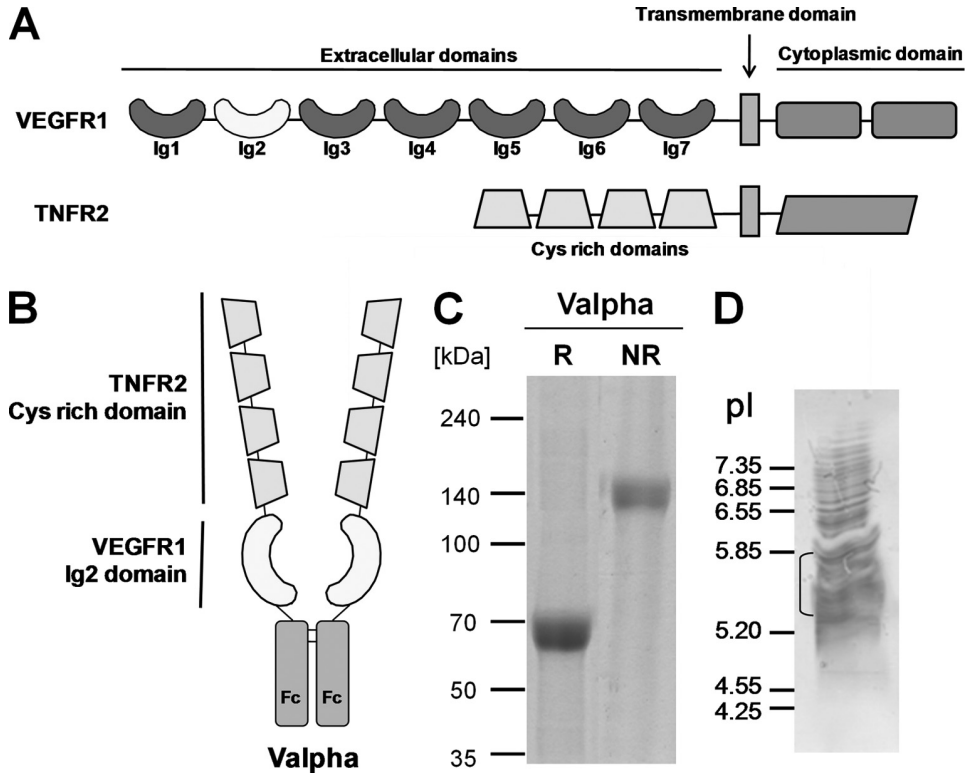

FIGURE 1. **Structure of the Valpha construct and characterization of purified Valpha protein.** *A*, schematic diagrams of the constructs showing human VEGFR1 and human TNFR2. *B*, the four cysteine-rich domains of TNFR2 essential for TNF-α binding are located in the N-terminal portion, Ig-like domain 2 (*Ig2*) of VEGFR1 is located in middle portion, and the Fc portion of human IgG is located in the C-terminal portion of Valpha. *C*, 2 μg of each reduced (*R*) and nonreduced (*NR*) Valpha protein was separated by SDS-PAGE and stained with Coomassie Blue. Molecular masses (in kilodaltons) are indicated on the left. *D*, 20 μg of Valpha protein was loaded on an IsoGel agarose isoelectric focusing plate and run at 50-mA constant current for 3 h. The gels were stained with Coomassie Blue. The *bracket* marks the pI range of the Valpha protein. Reference pI values are indicated on the left.

DTT, and 26% glycerol, and lysates were immunoblotted with anti-p65 antibody. The membrane was stripped and reprobed with anti-lamin antibody (Santa Cruz Biotechnology) for validation of equal loading of nuclear protein. To examine the inhibitory activity of Valpha on VEGF-A, human umbilical vein endothelial cells were cultured to confluence, and a scratch was made using a sterile blue tip (1000 μl) as described previously (39). Detached cells were removed, and dishes were treated with 2 μg/ml Fc, VEGF-Trap, Enbrel, or Valpha for 10 min and then treated with 50 ng/ml VEGF-A. Photographic images were taken at 0 and 24 h after treatment with VEGF-A for measurement of the migration distance. See supplemental "Methods" for more information.

RESULTS

Generation of Valpha—We designed and generated a novel fusion protein, Valpha, consisting of the cysteine-rich domains of human TNFR2, Ig-like domain 2 of human VEGFR1, and the Fc domain of human IgG (Fig. 1, *A* and *B*). The minimum ligand-binding domain of TNFR2 is located in the N-terminal portion, that of VEGFR1 is located in the middle portion, and the Fc domain of human IgG is located in the C-terminal portion of Valpha. The estimated molecular mass of Valpha is 65 kDa. Recombinant CHO cells expressing Valpha were established following a previously described method (38). Under reducing conditions, purified Valpha revealed predominantly single bands with the expected molecular masses of ~65 kDa (Fig. 1*C*). Under nonreducing conditions, the recombinant proteins were present as disulfide-linked dimers due to the presence of the Fc domain (Fig. 1*C*). Although the theoretical pI of Valpha is 7.14, its actual pI is ~5.5 (Fig. 1*D*).

In Vitro Characterization of Valpha—The ability of the recombinant Valpha protein to bind to VEGF-A and TNF-α *in vitro* was measured by ELISA (Fig. 2, *A* and *B*). The alternative ELISAs revealed that Valpha was capable of simultaneous binding to VEGF-A and TNF-α (Fig. 2, *C* and *D*). Surface plasmon resonance analyses revealed that Valpha proteins directly interacted with VEGF-A and TNF-α, and the K_D values for Valpha binding to VEGF-A and TNF-α were ~6.5 pM and ~64.1 nM, respectively (Fig. 3, *A* and *B*). Accordingly, Valpha almost completely inhibited TNF-α-induced NF-κB activation in primary cultured lymphatic endothelial cells (Fig. 4). Valpha also significantly reduced VEGF-A-induced migration of primary cultured blood endothelial cells and VEGFR2 phosphorylation *in vitro* (Fig. 5).

Valpha Pharmacokinetics—The pI of a recombinant protein affects its bioavailability and pharmacokinetics *in vivo*. Generally, proteins with high pI values display poor pharmacokinetic properties due to the fact that highly positively charged proteins are largely deposited at the site of subcutaneous injection, resulting from the nonspecific adhesion of highly negatively charged proteoglycans that compose the extracellular matrix (ECM) (9). We performed ECM binding assay with increasing

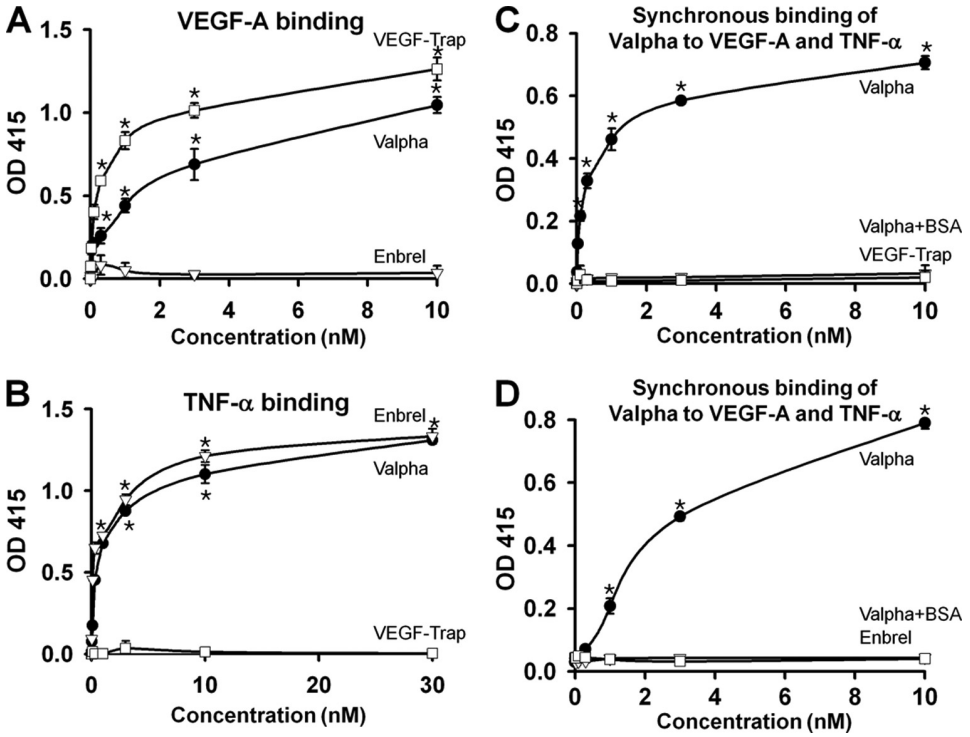

FIGURE 2. **Valpha can simultaneously interact with both VEGF-A and TNF-α.** The ability of Valpha to bind to VEGF-A and TNF-α was measured by ELISA. *A*, ELISA depicting the binding affinity for different concentrations (0.01–10 nM) of each indicated protein for VEGF-A. Values are given as means ± S.D. ($n = 4$). *, $p < 0.05$ *versus* Enbrel. *B*, ELISA depicting the binding affinity for different concentrations (0.03–30 nM) of each indicated protein for TNF-α. Values are given as means ± S.D. ($n = 4$). *, $p < 0.05$ *versus* VEGF-Trap. *C*, ELISA depicting simultaneous binding of Valpha to VEGF-A and TNF-α. 200 ng of TNF-α or BSA (negative control; *Valpha+BSA*) was coated on 96-well plates and blocked with 1% BSA in PBS. After washing, the indicated concentration of Valpha or VEGF-Trap was incubated and then washed. FLAG-tagged VEGF-A was added and captured with anti-FLAG M2 antibody. Values are given as means ± S.D. ($n = 4$). *, $p < 0.05$ *versus* VEGF-Trap. *D*, ELISA depicting simultaneous binding of Valpha to VEGF-A and TNF-α. 200 ng of VEGF-A or BSA (negative control; *Valpha+BSA*) was coated on 96-well plates and blocked with 1% BSA in PBS. After washing, the indicated concentration Valpha or Enbrel was incubated and then washed. His-tagged TNF-α was added and captured with HRP-conjugated anti-His tag antibody. Values are given as means ± S.D. ($n = 4$). *, $p < 0.05$ *versus* Enbrel.

concentrations of VEGF-Trap, Enbrel, or Valpha. In accordance with the theoretical pI values, the ECM binding of VEGF-Trap was relatively high, whereas Valpha showed less binding to the ECM (Fig. 3*C*). The ECM binding of Valpha was even less than that of Enbrel. For a standard pharmacokinetic analysis, mice were given single subcutaneous injections of 100 μg of VEGF-Trap, Enbrel, or Valpha (Fig. 3*D*). The proteins reached maximum levels in the blood at 1~2 h after injection, and their half-lives were ~2 days. Valpha had a maximum concentration of 7.88 ± 0.63 μg/ml and a total area under the curve concentration of 20.2 ± 1.88 μg × days/ml, VEGF-Trap had a maximum concentration of 6.18 ± 0.98 μg/ml and a total area under the curve concentration of 12.4 ± 1.62 μg × days/ml, and Enbrel had a maximum concentration of 8.04 ± 0.70 μg/ml and a total area under the curve concentration of 18.6 ± 2.04 μg × days/ml. Thus, the pharmacokinetic profiles were consistent with *in vitro* ECM adhesion properties, and in addition, Valpha had a relatively high bioavailability and excellent pharmacokinetic profile *in vivo*.

Valpha Reduces Pathological Vascular Tuft Formation and the Number of Macrophages in a Retinopathy Model—Retinopathy is a blinding disease with a hallmark of abnormal and excessive blood vessel growth that can cause retinal detachment (27). It is well known that VEGF-A plays a key role in developing diabetic retinopathy and age-related macular degeneration (7). Along with VEGF-A, TNF-α is an additional therapeutic target in treatment of retinopathy (40). Therefore, we hypothesized that double blockade of VEGF-A and TNF-α with Valpha could be more potent than single blockade of VEGF-A with VEGF-Trap. To observe the effect of Valpha as an anti-angiogenic and anti-inflammatory therapeutic molecule and to compare it with a single inhibitor of the VEGF-A or TNF-α pathway, we evaluated the ability of Valpha using an oxygen-induced retinopathy model that mimics diabetic retinopathy and age-related macular degeneration.

The number of retinal vascular tufts in the retinal vessels of oxygen-induced retinopathy (OIR), a typical feature of retinopathy, was highly increased in the Fc-treated group, whereas the number was significantly reduced in the Valpha- and VEGF-Trap-treated groups (Fig. 6). Similarly, we observed a large number of tortuous blood vessels, another pathological indication of retinopathy, in the Fc-treated group of OIR, whereas the tortuous blood vessels were hardly detected in the Valpha- and VEGF-Trap-treated groups of OIR (Fig. 6*B*). Quantification analysis revealed that OIR-induced formation of retinal vascular tufts (*white arrows*) caused by neovascularization in the retinal vessels was potently inhibited by treatment with Valpha, VEGF-Trap, or Enbrel (Fig. 6*C*). However, the number of $F4/80^+$ macrophages (*white arrowheads*) was similar in the VEGF-Trap- or Enbrel-treated group compared with the Fc-treated group, whereas the number was significantly reduced only in the Valpha-treated group (Fig. 6*D*). In addition, Valpha exerted a greater effect than the combined treatment with

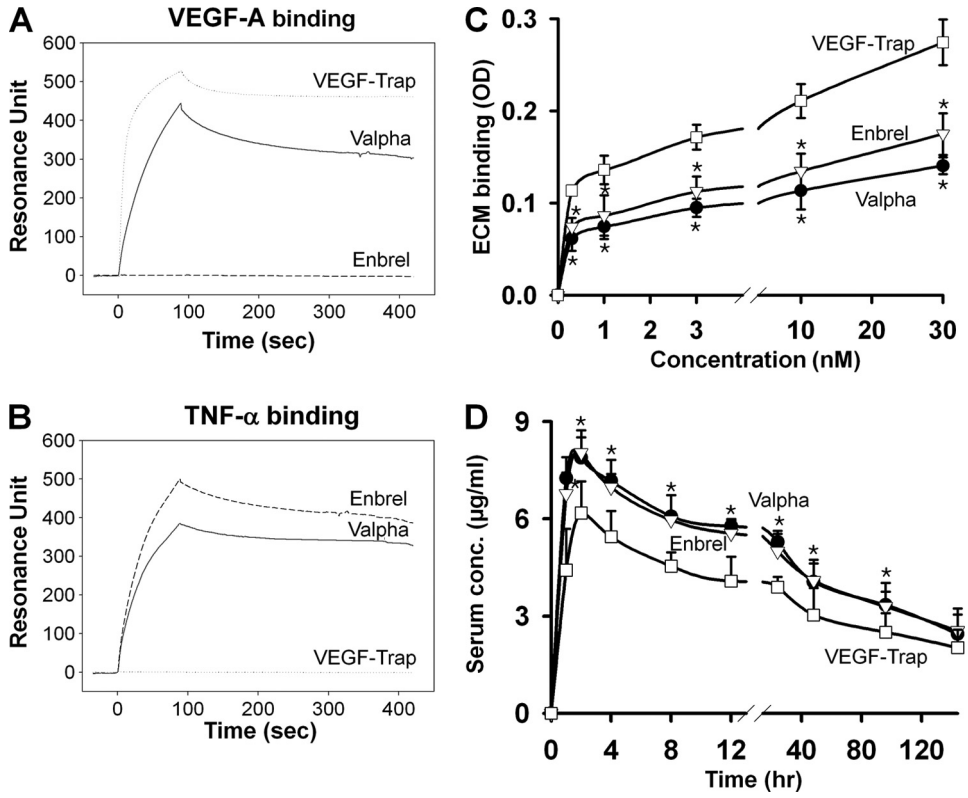

FIGURE 3. **Biacore analysis reveals interaction between Valpha and VEGF-A or TNF-α, and Valpha has low binding affinity for the ECM *in vitro* and displays an excellent pharmacokinetic profile *in vivo*.** *A* and *B*, sensorgrams for the association and dissociation of Valpha on immobilized VEGF-A (*A*) or TNF-α (*B*). Valpha proteins directly interacted with VEGF-A and TNF-α. *C*, ELISA depicting the binding affinity for different concentrations (0.3, 1, 3, 10, and 30 nM) of each indicated protein for the ECM. Values are given as means ± S.D. ($n = 4$). *, $p < 0.05$ *versus* VEGF-Trap. *D*, pharmacokinetic profiles. The indicated protein (5 mg/kg) was injected into C57BL/6 mice, and the serum levels of the proteins were measured. Values are given as means ± S.D. ($n = 4$). *, $p < 0.05$ *versus* VEGF-Trap.

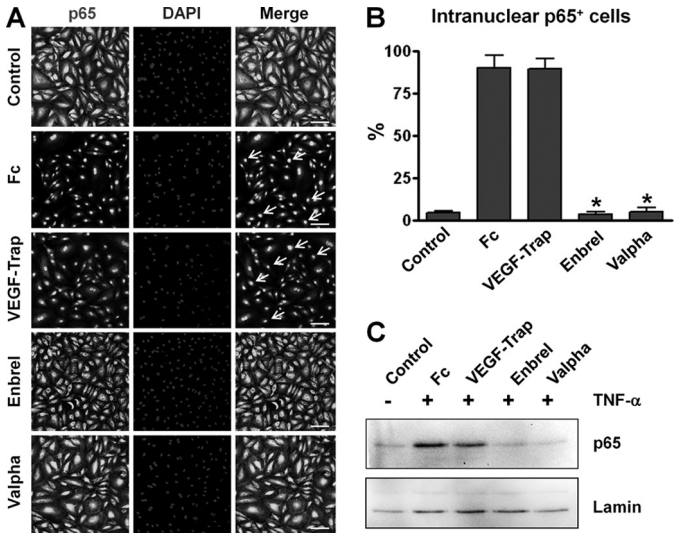

FIGURE 4. **Preincubation of Valpha markedly attenuates TNF-α-induced NF-κB activation in primary cultured LECs.** LECs were treated with PBS or 10 μg/ml Fc, VEGF-Trap, Enbrel, or Valpha for 15 min and then treated with TNF-α (10 ng/ml) for 30 min. *A*, for determination of NF-κB activation, nuclear translocalization of p65 (a subunit of NF-κB) was analyzed by immunostaining. Nuclei were counterstained with DAPI. *Arrows* indicate nuclear translocalization of p65. *Scale bars* = 100 μm. *B*, cells positive for p65 intranuclear staining (*white arrows* in *A*) were counted among 100 cells arbitrarily chosen in four different regions, and the values are presented as a percentage of the total cell number. *Bars* represent means ± S.D. ($n = 4$). *, $p < 0.05$ *versus* Fc. *C*, nuclear translocalization of p65 was detected by immunoblotting. Equal loading of nuclear protein was validated by immunoblotting of lamin in the same blot. Three independent experiments showed similar results.

VEGF-Trap and Enbrel in the reduction of F4/80$^+$ macrophage infiltration in the retina of OIR (supplemental Fig. S1).

Valpha Shows Relief Effects in a Psoriasis Model by Normalizing Epidermal Thickness and Vasculature Abnormalities—As VEGF-A and TNF-α play major roles in the pathogenesis of psoriasis, we applied Valpha to the psoriasis model using keratin 14-VEGF-A transgenic mice. The previously described protocol (33, 34) was slightly modified by challenging the sustained stimuli even during the protein treatment to maintain chronic inflammation, which is more clinically relevant than the protocol used earlier. TPA (0.02%) was applied during the protein treatment together with an injection of each protein following the first 2-week induction period (Fig. 7*A*). The treatment protocol was well tolerated in all mice. Serial TPA application to both sides of the right mouse ear resulted in progressively aggravated inflammation with erythematous and scaly skin with visible hyperplastic blood vessels, compared with acetone-only treatment of the left ear. After 2 weeks of the induction period, mice were randomly divided into four treatment groups. Then, according to treatment groups, Fc, VEGF-Trap, Enbrel, or Valpha was injected subcutaneously twice a week for 2 weeks, together with 0.02% TPA applications to both sides of the right ear. Compared with control Fc-treated mice, mice treated with VEGF-Trap, Enbrel, or Valpha exhibited a marked improvement of inflammatory signs both grossly and histologically (Fig. 7, *B* and *C*). Fc-treated mice also showed hyperplastic blood as well as an increased number of lymphatic vessels as

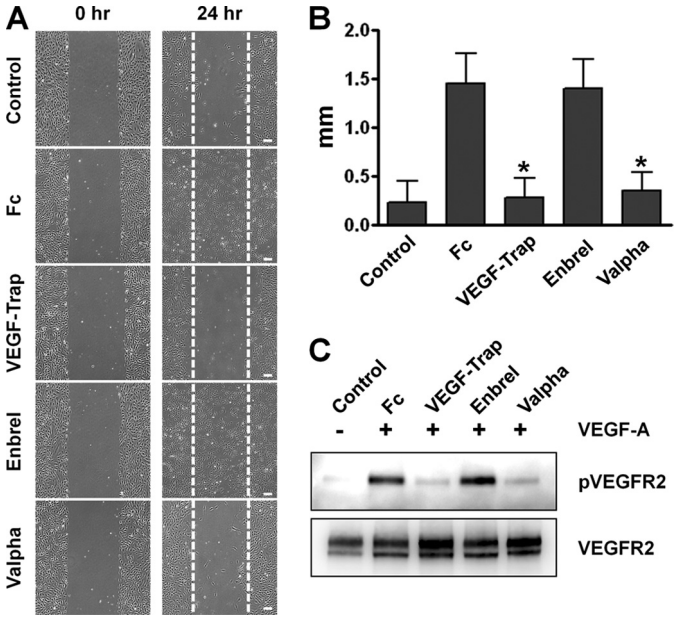

FIGURE 5. **Preincubation of Valpha markedly attenuates VEGF-A-induced migration of primary cultured human umbilical vein endothelial cells.** Human umbilical vein endothelial cells were treated with PBS or 2 μg/ml Fc, VEGF-Trap, Enbrel, or Valpha for 15 min and then treated with VEGF-A (50 ng/ml). *A*, photographic images were taken at 0 and 24 h after treatment with VEGF-A. *Scale bars* = 200 μm. *B*, distances of migrated cells from the starting borderline were measured, and the values are presented in millimeters. *Bars* represent means ± S.D. ($n = 4$). *, $p < 0.05$ *versus* Fc. *C*, 10 min after treatment with VEGF-A, the cells were harvested, and VEGFR2 phosphorylation was detected by immunoprecipitation and immunoblotting. Three independent experiments showed similar results.

demonstrated by immunofluorescence using anti-CD31 and anti-LYVE-1 antibodies, respectively (Fig. 7*D*). Subsequent image analyses revealed that Enbrel- or Valpha-treated mice showed significant improvements in epidermal thickness (Fig. 7*E*). Interestingly, Valpha showed superior therapeutic efficacy in epidermal thickness even when compared with Enbrel, although VEGF-Trap failed to produce a significant improvement in normalizing epidermal thickness (Fig. 7*E*). Furthermore, according to quantification analysis of the immunostaining results, Valpha significantly reduced the area of blood vessels as well as that of lymphatic vessels, which have been implicated in the pathogenesis of psoriasis (Fig. 7, *F* and *G*). Moreover, Valpha exerted greater anti-edema and anti-angiogenic activities than combined therapy of VEGF-Trap and Enbrel in the psoriasis mouse model (supplemental Fig. S2).

Valpha Shows Levels of Therapeutic Effects Similar to Those of Other Single Inhibitors in an Arthritis Model—Rheumatoid arthritis is the most common inflammatory arthritis, and suppression of angiogenesis may provide benefits in rheumatoid arthritis (35, 36). We generated collagen-induced arthritis models and tested the effect of Fc, VEGF-Trap, Enbrel, and Valpha in mice. The Fc-treated group developed severe swelling and erythema, whereas the mice treated with VEGF-Trap, Enbrel, or Valpha developed mild swelling and erythema in their hind paws (supplemental Fig. S3*A*). The collagen-induced arthritis severity can be determined using a clinical arthritis score and measurements of hind paw thickness. All parameters for the clinical course of collagen-induced arthritis indicated that arthritis was significantly attenuated with VEGF-Trap, Enbrel, or Valpha treatments compared with Fc treatment (supplemental Fig. S3, *B* and *C*). However, the degree of anti-arthritic effect of Valpha was similar to that of VEGF-Trap or Enbrel for the clinical arthritis score and hind paw thickness (supplemental Fig. S3, *B* and *C*).

DISCUSSION

In this study, we developed a novel chimeric decoy receptor (Valpha) that can simultaneously block the actions of VEGF-A and TNF-α related to diseases caused by inflammatory angiogenesis. Although Valpha was generated by fusion of two ligand-binding domains from different receptors, the recombinant engineered product still has the binding capability of its original counterparts, VEGF-A and TNF-α. Also, we found that Valpha significant blocks VEGF-A and TNF-α, as shown in *in vitro* cell-based assays and in subsequent *in vivo* therapeutic trials for treatment of retinopathy and psoriasis in mice.

To design the Valpha construct, we considered the minimum binding portion of original receptors and their biochemical characteristics. By fusion of the cysteine-rich domains of human TNFR2, Ig-like domain 2 of human VEGFR1, and the Fc domain of human IgG, we could generate a novel fusion protein that interacts with both VEGF-A and TNF-α with desirable biochemical profiles. Thus, the actual pI of Valpha is low enough to avoid attachment to the ECM, resulting in a more favorable pharmacokinetic profile *in vivo* compared with VEGF-Trap or Enbrel. Just as other therapeutic proteins have their unique pharmacokinetic profiles that lend to their critical factor of effectiveness, the low pI of Valpha is the key factor of importance. However, because VEGF-Trap and Enbrel have different biodistributions and half-lives in the body, they could not produce the same synergistic effects in the pathogenic environment. Furthermore, as a sole treatment agent, Valpha could be more cost-efficient for the patients than dual agents and will allow a more convenient administration of the treatment. Although Valpha has only a slightly better pharmacokinetic profile than Enbrel, the *in vivo* therapeutic effectiveness of Valpha was significantly better than that of Enbrel. In fact, our study showed that the effectiveness of Valpha was greater in anti-inflammatory, anti-edema, and anti-angiogenic activities than simultaneous therapy with VEGF-Trap and Enbrel. Thus, "double blockade" is the key factor responsible for the highly effective *in vivo* activity of Valpha. It is evident that Valpha has great benefits in relation to the engineered fusion antibody, which is a new trend in the current drug development field.

When we treated TNF-α on primary cultured lymphatic endothelial cells, NF-κB was activated and translocated into the nucleus. Although treatment with VEGF-Trap did not show any significant effect, nuclear translocation of NF-κB was dramatically inhibited in the Enbrel- or Valpha-treated group. These data show that Valpha could trap TNF-α as a decoy receptor in the cultured media and that TNF-α cannot bind to and activate its receptor. Meanwhile, VEGF-A-induced migration of primary cultured endothelial cells was significantly reduced only in the VEGF-Trap- or Valpha-treated group and not in the Enbrel-treated group. Taking an approach similar to that in the cell-based experiment using TNF-α, Valpha could also act as a decoy receptor for VEGF-A. Therefore, we con-

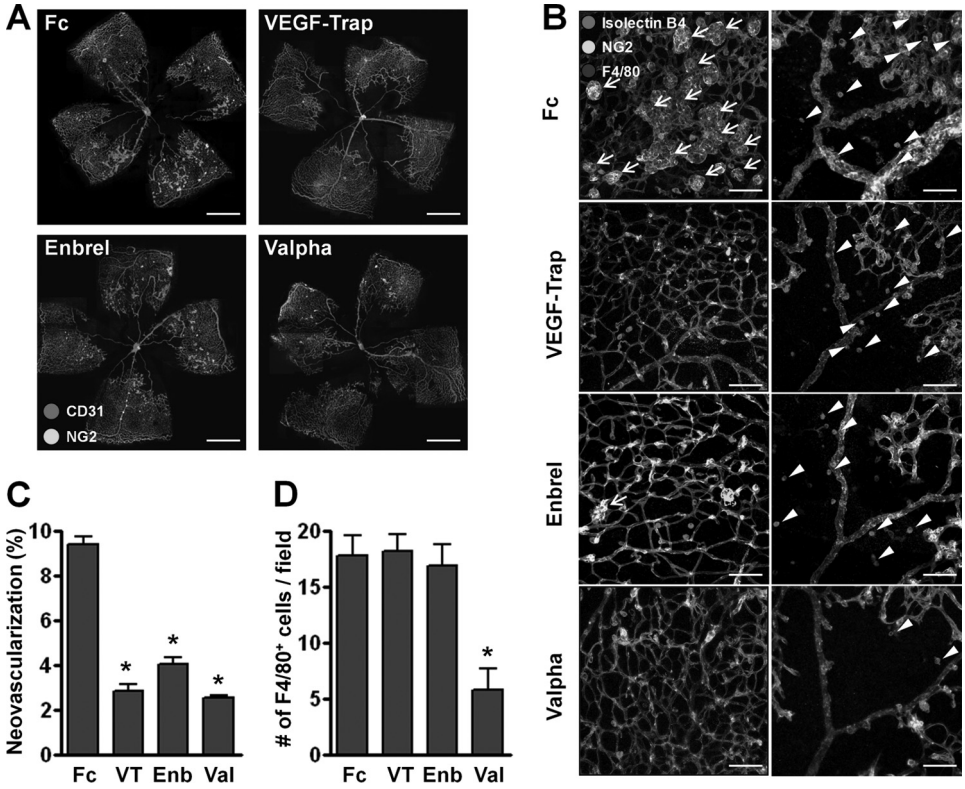

FIGURE 6. **Valpha shows relief effects in a mouse model of retinopathy.** At day 12 of OIR, the mice received intraocular injections of the indicated proteins (5 μg each) and killed on day 17 (P17), and the retinas were harvested. *A*, images showing CD31 and NG2 staining. The P17 retinal vasculature stained with CD31 showed the entire blood vessel pattern of the retina for each group. *Scale bars* = 1 mm. *B*, in this highly magnified mid-periphery region, vascular tufts and the number of F4/80$^+$ macrophages were dramatically reduced by introducing Valpha protein. *Arrows* indicate vascular tufts. *Arrowheads* indicate F4/80$^+$ macrophages. *Scale bars* = 100 μm. *C*, quantification analysis of neovascularization is presented as a percentage. *Bars* represent means ± S.D. ($n = 4$). *, $p < 0.05$ *versus* Fc. *D*, cells positive for F4/80$^+$ staining were counted arbitrarily chosen in four different regions, and the values are presented as the cell number per field. *Bars* represent means ± S.D. ($n = 4$). *, $p < 0.05$ *versus* Fc. *VT*, VEGF-Trap; *Enb*, Enbrel; *Val*, Valpha.

clude that TNF-α and VEGF-A signaling pathways can be blocked by treatment with Valpha. Because of the promising results from cell-based functional assays *in vitro*, we next tested the *in vivo* effect of Valpha using mice disease models.

Our results from the retinopathy experiment indicated that Valpha had an excellent therapeutic effect in reducing the number of abnormal vascular tufts, similar to VEGF-Trap. As abnormal vascular tufts are easily detected in pathological conditions of the retina, normalization of those irregular vessel structures reflects a quite favorable outcome of retinopathy treatment (28, 29). From treatment outcomes of VEGF-Trap and Valpha, which have a common target to be sequestrated, VEGF-A, it was shown that blockade of VEGF-A signaling is enough to reduce pathological vascular tufts in retinopathy. Interestingly, the number of F4/80$^+$ macrophages was significantly decreased in the Valpha-treated group, whereas the results in the VEGF-Trap- and Enbrel-treated groups were not significant different from those in the Fc-treated group. Therefore, single inhibition of VEGF-A or TNF-α separately is not sufficient for blockade of macrophage infiltration, but simultaneous blockade of both VEGF-A and TNF-α using Valpha is a promising strategy for blocking macrophage infiltration. Although the remaining macrophages in the Fc-, VEGF-Trap-, and Enbrel-treated groups might induce further pathological inflammatory responses in the retina and thereby accelerate disease progression, our data indicate that Valpha is more effective than VEGF-Trap or Enbrel for treating retinopathy in mice due to its ability to block macrophage infiltration. Also, there are several reports that a decoy receptor for VEGF-A repressed not only pathological but also physiological neovascularization, and so a single treatment with VEGF-Trap may not be the ideal method of retinopathy treatment (11, 41). Thus, simultaneous blockade of both VEGF-A and TNF-α to reduce both abnormal vessels and macrophages should be considered in future application for efficient treatment of ocular diseases.

In addition, we examined whether Valpha treatment could ameliorate chronic inflammation in a mouse model of psoriasis. The pathophysiology of psoriasis is not well understood, but increasing evidence indicates that TNF-α is a crucial cytokine implicated in psoriasis pathogenesis, and biological therapies targeting TNF-α have revolutionized the treatment of patients with severe psoriasis. Albeit very effective, these biological agents have little influence on the actual production of TNF-α by the immune cells or keratinocytes, which might be associated with recurrence of the disease after cessation of therapy (42). On the other hand, VEGF-A has been another focus of intense research in psoriasis pathogenesis and treatment. Patients with psoriasis show an increased expression of VEGF-A in both skin lesions and serum, and polymorphisms in VEGF and VEGFR genes are associated with psoriasis susceptibility, severity, and prognosis (42, 43). Furthermore, VEGF-A antagonism leads to the reversal of disease phenotypes in

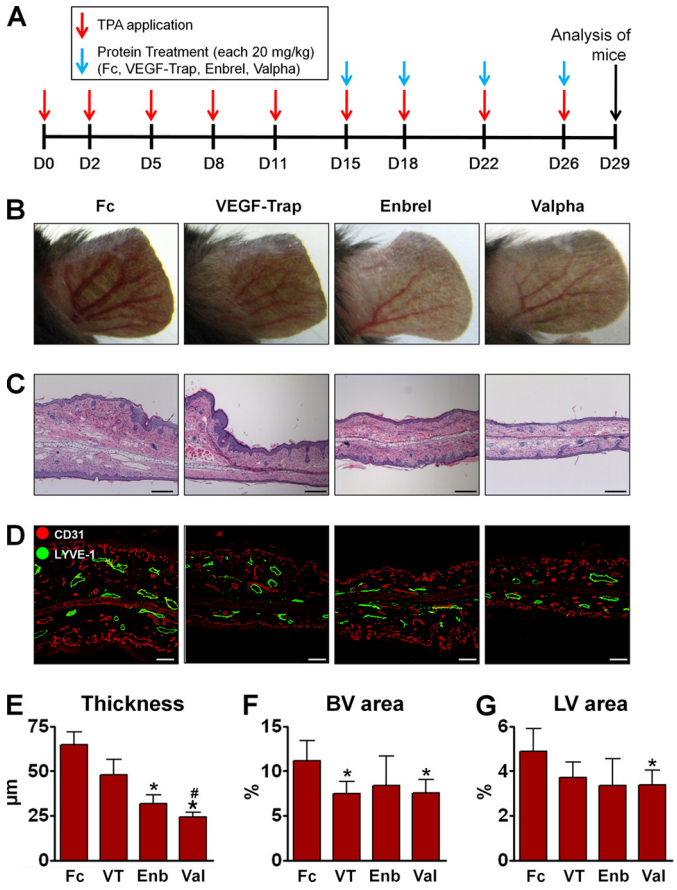

FIGURE 7. **Valpha alleviates inflammation in a mouse model of psoriasis by normalizing the hyperplastic epidermis and vascular abnormalities.** *A*, experimental scheme of a TPA-induced psoriasis model using keratin 14-VEGF-A mice for two periods: one includes five topical application of 0.02% TPA to both sides of the ear for 2 weeks (induction period), and one includes treatment with each indicated protein twice a week for 2 weeks (treatment period). TPA was applied during the treatment period as well as the induction period. *D*, day. *B–D*, after generation of TPA-induced psoriasis, mouse ears were examined. *B*, the gross appearance of TPA-treated ears at the end of the study (a 2-week induction period followed by a 2-week treatment period using each indicated protein) showed prominently enlarged hyperplastic blood vessels on the erythematous and scaly ear skin of Fc-treated mice, whereas VEGF-Trap-, Enbrel-, or Valpha-treated mice showed lower degrees of inflammatory signs. *C*, hematoxylin/eosin staining of TPA-treated ears revealed that, compared with Fc-treated mice, which showed psoriasis-like histological changes such as acanthosis, parakeratosis, and mixed inflammatory infiltrates, VEGF-Trap-, Enbrel-, or Valpha-treated mice showed significant improvements in these phenotypes. *Scale bars* = 200 μm. *D*, immunofluorescence analysis using anti-CD31 (*red*) and anti-LYVE-1 (*green*) antibodies showed blood and lymphatic vessels, respectively, after treatment with each indicated protein. *Scale bars* = 100 μm. *E–G*, quantification analyses of ear thickness (in micrometers), blood vessel (*BV*) area (percent), and lymphatic vessel (*LV*) area (%). *Bars* represent means ± S.D. ($n = 3$). *, $p < 0.05$ *versus* Fc; #, $p < 0.05$ *versus* Enbrel. *VT*, VEGF-Trap; *Enb*, Enbrel; *Val*, Valpha.

mouse models of psoriasis (31, 32, 44, 45). To assess the combinatorial efficacy by double blockade of VEGF-A and TNF-α, we employed the psoriasis model previously characterized as Th17-driven psoriasis-like inflammation with elevated levels of VEGF-A and TNF-α in skin (33). Despite concurrent TPA challenges, Valpha produced a dramatic and significant improvement in epidermal hyperplasia compared with Fc, VEGF-Trap, and even Enbrel (Fig. 7*E*). Moreover, unlike VEGF-Trap-treated mice, which showed a significant decrease only in the area of blood vessels, Valpha-treated mice showed significant improvements in the area of blood and lymphatic vessels. In particular, Valpha was the only treatment that produced a significant improvement in the area of lymphatic vessels, even when blockade of either cytokine separately failed to produce a significant change. Thus, the double blockade of VEGF-A and TNF-α using Valpha is a far superior strategy than single blockade of either cytokine by normalizing epidermal thickness and vascular abnormalities. In addition to all the pathological benefits of Valpha, the high bioavailability and excellent pharmacokinetic profile of Valpha *in vivo* might even contribute to better efficacy because limited access to the target tissue of conventional drugs is a barrier to efficient treatment (45).

Inflammatory angiogenesis is a hallmark and a critical contributing factor in the progression of rheumatoid arthritis (36). Therefore, inhibition of inflammatory angiogenesis using Valpha could be an effective method to reduce the progression and joint destruction of rheumatoid arthritis. Although we had originally expected that Valpha possessed a synergistic or additive effect in treatment of arthritis, there was no marked or observable difference in the effectiveness between Valpha and other single inhibitors. In general, the exact amounts and balance of VEGF-A and TNF-α affecting the pathogenesis of a certain disease might be varied depending on the types of diseases. It is important to note that although a double blocker is much more effective than a single blocker in many disease models as shown in cases of retinopathy and psoriasis, the efficacy of the double blocker can sometimes be different for other types of diseases that are caused by other unknown factors.

Valpha, the chimeric double decoy receptor that binds to both VEGF-A and TNF-α and blocks their functionality, is a highly promising therapeutic molecule for the treatment of retinopathy and psoriasis. In addition, if further clinical studies of Valpha are performed, it is quite possible that Valpha can be the next dominant treatment for other diseases caused by pathological inflammatory angiogenesis. In addition to the therapeutic effects of Valpha, the other benefits of Valpha are that it is a cost-efficient alternative to double application of separate drugs and that it is convenient for both the patient and administrator.

REFERENCES

1. Ferrara, N., and Kerbel, R. S. (2005) *Nature* **438,** 967–974
2. Ferrara, N., Gerber, H. P., and LeCouter, J. (2003) *Nat. Med.* **9,** 669–676
3. Shibuya, M., and Claesson-Welsh, L. (2006) *Exp. Cell Res.* **312,** 549–560
4. Folkman, J. (2007) *Nat. Rev. Drug Discov.* **6,** 273–286
5. Carmeliet, P. (2003) *Nat. Med.* **9,** 653–660
6. De Bandt, M., Ben Mahdi, M. H., Ollivier, V., Grossin, M., Dupuis, M., Gaudry, M., Bohlen, P., Lipson, K. E., Rice, A., Wu, Y., Gougerot-Pocidalo, M. A., and Pasquier, C. (2003) *J. Immunol.* **171,** 4853–4859
7. Aiello, L. P. (2005) *N. Engl. J. Med.* **353,** 839–841
8. Ferrara, N., Hillan, K. J., Gerber, H. P., and Novotny, W. (2004) *Nat. Rev. Drug. Discov.* **3,** 391–400
9. Holash, J., Davis, S., Papadopoulos, N., Croll, S. D., Ho, L., Russell, M., Boland, P., Leidich, R., Hylton, D., Burova, E., Ioffe, E., Huang, T., Radziejewski, C., Bailey, K., Fandl, J. P., Daly, T., Wiegand, S. J., Yancopoulos, G. D., and Rudge, J. S. (2002) *Proc. Natl. Acad. Sci. U.S.A.* **99,** 11393–11398
10. Hurwitz, H., Fehrenbacher, L., Novotny, W., Cartwright, T., Hainsworth, J., Heim, W., Berlin, J., Baron, A., Griffing, S., Holmgren, E., Ferrara, N., Fyfe, G., Rogers, B., Ross, R., and Kabbinavar, F. (2004) *N. Engl. J. Med.* **350,** 2335–2342

11. Ng, E. W., Shima, D. T., Calias, P., Cunningham, E. T., Jr., Guyer, D. R., and Adamis, A. P. (2006) *Nat. Rev. Drug. Discov.* **5,** 123–132
12. Byrne, A. T., Ross, L., Holash, J., Nakanishi, M., Hu, L., Hofmann, J. I., Yancopoulos, G. D., and Jaffe, R. B. (2003) *Clin. Cancer Res.* **9,** 5721–5728
13. Saishin, Y., Saishin, Y., Takahashi, K., Lima e Silva, R., Hylton, D., Rudge, J. S., Wiegand, S. J., and Campochiaro, P. A. (2003) *J. Cell Physiol.* **195,** 241–248
14. Verheul, H. M., Hammers, H., van Erp, K., Wei, Y., Sanni, T., Salumbides, B., Qian, D. Z., Yancopoulos, G. D., and Pili, R. (2007) *Clin. Cancer Res.* **13,** 4201–4208
15. Hickey, M. J., Reinhardt, P. H., Ostrovsky, L., Jones, W. M., Jutila, M. A., Payne, D., Elliott, J., and Kubes, P. (1997) *J. Immunol.* **158,** 3391–3400
16. Rojanasakul, Y., Ye, J., Chen, F., Wang, L., Cheng, N., Castranova, V., Vallyathan, V., and Shi, X. (1999) *Mol. Cell. Biochem.* **200,** 119–125
17. Karin, M., and Lin, A. (2002) *Nat. Immunol.* **3,** 221–227
18. Taylor, P. C. (2001) *Curr. Opin. Rheumatol.* **13,** 164–169
19. Peppel, K., Crawford, D., and Beutler, B. (1991) *J. Exp. Med.* **174,** 1483–1489
20. Shibuya, M. (2001) *Int. J. Biochem. Cell Biol.* **33,** 409–420
21. Ruch, C., Skiniotis, G., Steinmetz, M. O., Walz, T., and Ballmer-Hofer, K. (2007) *Nat. Struct. Mol. Biol.* **14,** 249–250
22. Jung, K., Lee, J. E., Kim, H. Z., Kim, H. M., Park, B. S., Hwang, S. I., Lee, J. O., Kim, S. C., and Koh, G. Y. (2009) *PLoS ONE* **4,** e7403
23. Vandenabeele, P., Declercq, W., Beyaert, R., and Fiers, W. (1995) *Trends Cell Biol.* **5,** 392–399
24. Schall, T. J., Lewis, M., Koller, K. J., Lee, A., Rice, G. C., Wong, G. H., Gatanaga, T., Granger, G. A., Lentz, R., and Raab, H. (1990) *Cell* **61,** 361–370
25. Tartaglia, L. A., Pennica, D., and Goeddel, D. V. (1993) *J. Biol. Chem.* **268,** 18542–18548
26. Saint-Geniez, M., and D'Amore, P. A. (2004) *Int. J. Dev. Biol.* **48,** 1045–1058
27. Smith, L. E., Wesolowski, E., McLellan, A., Kostyk, S. K., D'Amato, R., Sullivan, R., and D'Amore, P. A. (1994) *Invest. Ophthalmol. Vis. Sci.* **35,** 101–111
28. Chen, J., Connor, K. M., Aderman, C. M., and Smith, L. E. (2008) *J. Clin. Invest.* **118,** 526–533
29. Skoura, A., Sanchez, T., Claffey, K., Mandala, S. M., Proia, R. L., and Hla, T. (2007) *J. Clin. Invest.* **117,** 2506–2516
30. Lowes, M. A., Bowcock, A. M., and Krueger, J. G. (2007) *Nature* **445,** 866–873
31. Xia, Y. P., Li, B., Hylton, D., Detmar, M., Yancopoulos, G. D., and Rudge, J. S. (2003) *Blood* **102,** 161–168
32. Schonthaler, H. B., Huggenberger, R., Wculek, S. K., Detmar, M., and Wagner, E. F. (2009) *Proc. Natl. Acad. Sci. U.S.A.* **106,** 21264–21269
33. Hvid, H., Teige, I., Kvist, P. H., Svensson, L., and Kemp, K. (2008) *Int. Immunol.* **20,** 1097–1106
34. Teige, I., Hvid, H., Svensson, L., Kvist, P. H., and Kemp, K. (2009) *J. Invest. Dermatol.* **129,** 1437–1445
35. Firestein, G. S. (2003) *Nature* **423,** 356–361
36. Lainer-Carr, D., and Brahn, E. (2007) *Nat. Clin. Pract. Rheumatol.* **3,** 434–442
37. Nagashima, M., Yoshino, S., Aono, H., Takai, M., and Sasano, M. (1999) *Clin. Exp. Immunol.* **116,** 360–365
38. Hwang, S. J., Choi, H. H., Kim, K. T., Hong, H. J., Koh, G. Y., and Lee, G. M. (2005) *Protein Expr. Purif.* **39,** 175–183
39. Kim, H. Z., Jung, K., Kim, H. M., Cheng, Y., and Koh, G. Y. (2009) *Biochim. Biophys. Acta* **1793,** 772–780
40. Gardiner, T. A., Gibson, D. S., de Gooyer, T. E., de la Cruz, V. F., McDonald, D. M., and Stitt, A. W. (2005) *Am. J. Pathol.* **166,** 637–644
41. Ishida, S., Usui, T., Yamashiro, K., Kaji, Y., Amano, S., Ogura, Y., Hida, T., Oguchi, Y., Ambati, J., Miller, J. W., Gragoudas, E. S., Ng, Y. S., D'Amore, P. A., Shima, D. T., and Adamis, A. P. (2003) *J. Exp. Med.* **198,** 483–489
42. Chua, R. A., and Arbiser, J. L. (2009) *Autoimmunity* **42,** 574–579
43. Young, H. S., Summers, A. M., Read, I. R., Fairhurst, D. A., Plant, D. J., Campalani, E., Smith, C. H., Barker, J. N., Detmar, M. J., Brenchley, P. E., and Griffiths, C. E. (2006) *J. Invest. Dermatol.* **126,** 453–459
44. Halin, C., Fahrngruber, H., Meingassner, J. G., Bold, G., Littlewood-Evans, A., Stuetz, A., and Detmar, M. (2008) *Am. J. Pathol.* **173,** 265–277
45. Kunstfeld, R., Hirakawa, S., Hong, Y. K., Schacht, V., Lange-Asschenfeldt, B., Velasco, P., Lin, C., Fiebiger, E., Wei, X., Wu, Y., Hicklin, D., Bohlen, P., and Detmar, M. (2004) *Blood* **104,** 1048–1057